Scenedesmus regularis: An alternative biosorbent for the efficient and fast removal of methylene blue

Kankılıç G. B.*
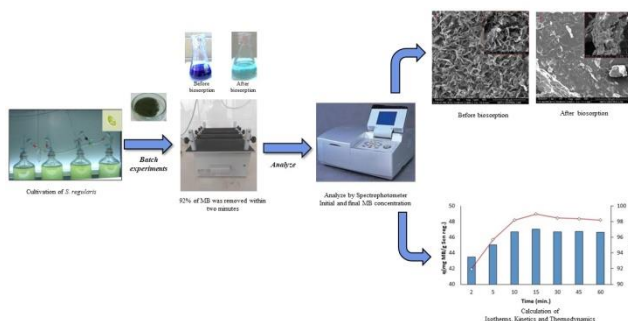
Department of Biology, Faculty of Arts and Sciences, Kırıkkale University, 71450 Yahşihan, Kırıkkale, Turkey
*to whom all correspondence should be addressed: e-mail: gokbenbasaran@gmail.com; gokbenbasaran@kku.edu.tr

Graphical Abstract

Abstract

This study focused on removing methylene blue (MB) from aqueous solutions using microalga *Scenedesmus regularis* as a biosorbent. The biomass was characterized by Fourier transform infrared spectroscopy (FT-IR) and field emission scanning electron microscopy (FE-SEM). The difference in thermal properties of the biomass was investigated by thermogravimetric analysis (TGA). The adsorption capacity of *S. regularis* was tested with different environmental key parameters (pH, temperature, biosorbent dosage, dye concentration, and contact time) in batch system experiments. The maximum adsorption capacity was 341.34 mg/g at a pH of 6.8, a temperature of 25 °C, a dye concentration of 250 mg/L, and a biosorbent concentration of 5 mg. Approximately 92% of the dye was removed within two minutes, and the removal efficiency reached 99% within 15 minutes. MB adsorption equilibrium data fit well with the Langmuir (R^2=0.994) and Dubinin-Radushkevich (R^2=0.993) isotherm models. The kinetic model of adsorption followed pseudo-second-order kinetics. Thermodynamic parameters showed that the adsorption process was endothermic and physical, favorable, and spontaneous. The results showed that *S. regularis* is an eco-friendly biosorbent with efficient performance that may be used for MB removal without any modification.

Key Words: Microalgae, Adsorption, Toxic dyes, Isotherm, Kinetics, Thermodynamic

1. Introduction

Water, which is crucial for life and ecosystems, is contaminated and exhausted day by day, both within the world and in our country, due to the expanding human population, worldwide climate change, industrial contamination, and uncontrolled domestic and hazardous chemical wastes. Increasing pollution levels of water resources, which are not evenly distributed globally, make it challenging to reach accessible, quality, and qualified water resources for all living creatures. Among the environmental pollutants discharged into aquatic ecosystems, dyes and toxic heavy metals are significant concerns (Shooto *et al.*, 2019).

Dyes are commonly used in various industries, such as textile, paper, pulp, painting, printing, cosmetics, plastics, and pharmaceutics (Ahmad *et al.*, 2009; Ravikumar *et al.*, 2005). Over 100,000 dyes are commercially available, and approximately 15% of the annual production is discharged into aquatic environments without any treatment or partial treatment (Kumar *et al.*, 2013; Rangabhashiyam *et al.*, 2018). The complex aromatic structures and colors of synthetic dyes worsen water quality parameters such as biological oxygen demand, chemical oxygen demand, suspended solids, and total dissolved solids and thereby reduce photosynthetic activity, impairing ecological balance in the aquatic environment (Ahmad *et al.*, 2016; Rangabhashiyam *et al.*, 2018). At the same time, the carcinogenic, mutagenic, and potentially toxic effects of dye molecules on all living organisms in the food chain make them an important research area for the aquatic environment (Baruah *et al.*, 2017; Kabra *et al.*, 2011). Even if dyes are mixed with minimal amounts in aquatic systems, they are also aesthetically undesirable due to their high visibility and low degradation rates (Mohebali *et al.*, 2018).

As a toxic water-soluble cationic dye, MB is significantly used in coloring textile products, papers, plastics, and impermanent hair colorants. (Baruah *et al.*, 2017; Shooto *et al.*, 2020). The adverse effects of MB comprise eye injury, inhalation problems, gastroenteritis, queasiness, vomiting, heartbeat increase, mental confusion, and tissue necrosis (Dahri *et al.*, 2015; Mitrogiannis *et al.*, 2015; Rafatullah *et al.*, 2010). Based on the adverse effects of MB, researchers have focused on removal techniques. Although many methods are used to remove pollutants (such as

coagulation, ozonation, electrolysis, cation exchange membranes, electrochemical degradation, sonochemical degradation, and enhanced ultrafiltration), adsorption is the most preferred (Gokulan *et al.*, 2022a). Due to its simplicity, ease of application, efficiency, flexibility, low energy requirement, and economically profitable (Rafatullah *et al.*, 2010; Rahman *et al.*, 2020; Rajasulochana and Preethy, 2016; Wang *et al.*, 2005).

To date, several biosorbents have been used for MB removal from aqueous solutions, such as aquatic plants (Kankılıç *et al.*, 2016), macroalgae (Aravindhan *et al.*, 2007), lichens (Koyuncu and Kul, 2020), fungi (Naghipour *et al.*, 2016), ginger root (Shooto *et al.*, 2019), banana, cucumber, potato peels (Stavrinou *et al.*, 2018), and microalgae (Lebron *et al.*, 2018).

Among several biosorbents, microalgae have a special place because of their wide distribution in different geographical regions and the potential for cultivation anywhere from freshwater to saltwater. Microalgae have a wide tolerance to varied environmental factors, such as pH, temperature, turbidity, O_2, and CO_2 levels, resulting in low-cost production (Gualtieri and Barsanti, 2006; Sari *et al.*, 2011). Even though the studies on the removal of MB are prevalent, microalgae as easy access, low-cost, and eco-friendly biomass is highly considerable in creating practical potential with future anticipatory. *Scenedesmus* is a very common, easily accessible microalgae genus in freshwater ecosystems. They can develop in profoundly contaminated aquatic systems and are ordinarily utilized as contamination markers (Phinyo *et al.*, 2017). At this point, the *Scenedesmus* genus can be used as a good candidate for removing environmental pollutants.

The present work's objective was set to investigate the effectiveness of *Scenedesmus regularis* as a biosorbent for the removal of the extensively used dye MB. Within this scope, the adsorptive properties of *S. regularis* were optimized according to the different environmental vital factors, and maximum removal efficiency was investigated. The adsorption process was evaluated with thermodynamic, kinetic, and isotherm models.

2. Materials and methods

2.1. Microalgae and culture media

Scenedesmus regularis is a green microalga species belonging to the Chlorophyta phylum. The species was isolated from the Kızılırmak River (Kırıkkale, Turkey). As explained in Kankılıç et al. (2020), the collected biomass was cultivated. After cultivation, morphological characterization of the biomass was estimated. Molecular identification of *Scenedesmus regularis* was made by PCR amplification of 18S rRNA and ITS gene regions to confirm characterization. Sequence results were compared with the GenBank database for similarity assessment.

The algal biomass was collected in the middle of the stationary phase (≈ 15th day) by centrifugation at 3000 rpm for 15 min. The collected biomass was dried in a drying oven at 40 °C (Binder™ Classic. Line Drying Oven, Series ED).

2.2. Chemicals/reagents

Methylene blue ($C_{16}H_{18}ClN_3S\cdot 3H_2O$, the synthetic dye) was a commercially available product from Sigma Aldrich (Saint Louis, MO, USA). MB solutions at different concentrations were prepared in MilliQ water; the pH of the aqueous solution was adjusted to the working pH using 0.1 M NaOH or 0.1 M HCl.

2.3. Characterization

FTIR analyses of *S. regularis* before and after adsorption were performed using a Bruker (IFS 66/S model) FTIR spectrometer (wavenumber range: 400–4000 cm^{-1}).

Field emission scanning electron microscopy (FE-SEM/QUANTA 400F) was used to determine the microstructure of raw and MB-loaded *S. regularis.*

Thermal properties of the raw and MB-loaded biomass were investigated by TGA, Q500 (USA) model analyzer. Measurements were performed at a heating rate of 10 °C/min, a temperature range of 30-600 °C under a nitrogen atmosphere, and 10 ml/min a gas flow rate.

2.4. Adsorption studies

Methylene blue removal experiments were conducted in a 50 mL Erlenmeyer flask batch system. The effects of selected parameters, pH (2-10), contact time (2-60 min), ambient temperature (5-40 °C), biosorbent dosage (1–6 mg), and initial dye concentration (5–250 mg/L), on the adsorption capacity of *S. regularis,* were evaluated. Each adsorption experiment was performed under conditions where one parameter was changed at a time while the other parameters were kept constant. After each adsorption process, the supernatant was removed by filtration. Quantitation of the remaining MB concentration was carried out with a SpectroScan 80 DV spectrophotometer at 665 nm, the absorption maxima of MB, using a calibration curve. Samples were diluted appropriately to keep absorbance values in the linear reference range of the curve.

The amount of dye adsorbed by *S. regularis* biomass and the removal efficiency was calculated in Eqs. (1) and (2), respectively.

$$q_e = (C_o - C_e)\, V/m \qquad\qquad\qquad (1)$$

$$\text{Dye removal efficiency (\%)} = (C_o - C_e/C_o) \times 100 \qquad (2)$$

where q_e is the adsorption capacity in milligrams per gram; C_o and C_e are the initial and final dye concentrations after treatment for certain periods (mg/L), respectively; V is the volume of MB solution in ml, and m is the total amount of biosorbent in grams.

The equilibrium conditions of the adsorption process were assessed with Langmuir, Freundlich, and Dubinin-Radushkevich (D-R) isotherm models. Pseudo-first-order and pseudo-second-order kinetic models were used for the determination of kinetic behaviors. Thermodynamic parameters, such as Gibbs free energy (ΔG°), enthalpy (ΔH°), and entropy (ΔS°), were calculated to elaborate the adsorption process. The parameters were calculated with following equations (Saha *et al.*, 2011; Gokulan *et al.*, 2020; Kankılıç *et al.*, 2020).

$$\Delta G^o = -RT \ln Kd \tag{3}$$

$$\Delta G^o = \Delta H^o - T\Delta S^o \tag{4}$$

$$\ln Kd = -\Delta G^o/RT = \Delta S^o/R - \Delta H/RT \tag{5}$$

3. Results and discussion

3.1. Characterization of Scenedesmus regularis

The FT-IR spectra of MB, raw, and MB-loaded *S. regulari*s biomass are shown in Figure 1. The functional groups of raw and MB-loaded biomass alterations were analyzed using a Bruker IFS 66/S model. The broadband at approximately 3300 cm^{-1} is characteristic of OH groups, and this vibration shows that the *S. regularis* surface has a significant number of alcoholic and phenolic -OH groups (Baruah *et al.*, 2017; Kankılıç *et al.*, 2016). The peak observed at 2920 cm^{-1} was related to the aliphatic groups' C–H stretching vibrations (Daneshvar *et al.*, 2017). The absorption bands at 1035 and 1058 cm^{-1} correspond to C–O and C–C–O stretching vibrations and refer to cellulose derivatives as well as alcohols, ethers, and carboxylic acids (Lebron *et al.*, 2018). After MB adsorption, the new absorption bands observed at 1598, 1386, and 1328 cm^{-1} could be attributed to the S=O groups of sulfonamides originating from MB (Baruah *et al.*, 2017). Also, the absorption band at the 1386 cm^{-1} could correspond to -CH$_3$ bending vibration (Mohebali *et al.*, 2018). These functional groups on the *S. regularis* surface have a significant role in MB adsorption (Daneshvar *et al.*, 2017). According to Figure 1, some of the peaks have shifted or disappeared, while some new peaks have developed. The absorption peaks were moved to a higher frequency region due to dye molecules packing the surface of the biosorbent.
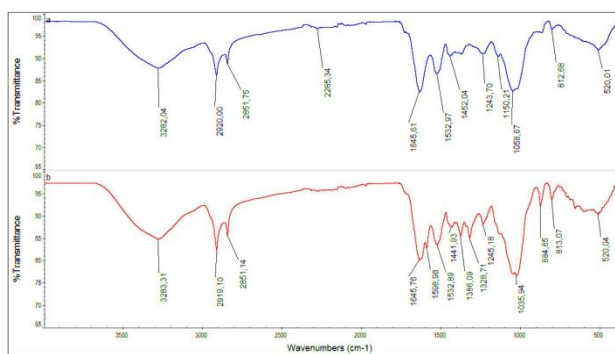

Figure 1. FTIR spectra of *S. regularis*: (a) raw; (b) MB loaded.

FE-SEM images were taken to show differences in microstructure between raw and MB-loaded *S. regularis* (Figure 2). FE-SEM images showed that the surface morphology of raw and MB-loaded biomass varied significantly. After adsorption, the pores were full of MB. Accumulation of the dye molecules has taken place at the biomass surface, indicating the dye adsorption site.
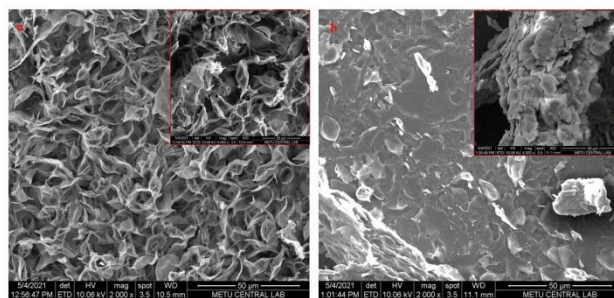

Figure 2. FE-SEM micrographs of *S. regularis*: (a) raw, (b) MB loaded.

The thermal stability of MB, *S. regularis*, and MB-loaded *S. regularis* was evaluated at various temperatures by TGA. The TGA curve of MB showed small weight losses below 100 ºC due to evaporation of moisture (Figure 3.). According to the thermograms, *S. regularis* and MB loaded *S. regularis* have one degradation step at around 306 and 312 ºC, respectively. After MB adsorption it has been seen that the degradation temperature was a trace increased. While comparing the residue values it can be seen that adsorption has occurred on the biomass surface. The residue of MB was highest and *S. regularis* was lowest. The MB-loaded *S. regularis* residue was approximately 10% higher than the raw biomass, demonstrating that the adsorption took place physically (Figure 3).
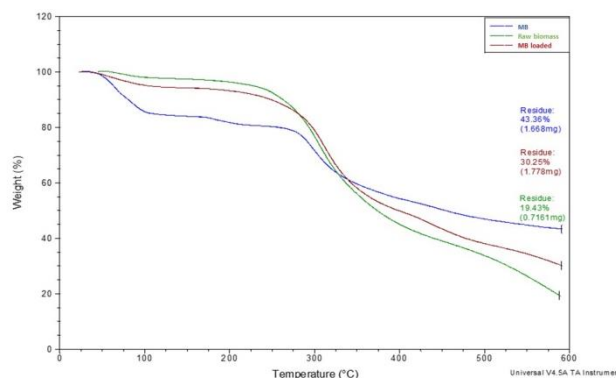

Figure 3. TGA curves of MB, raw biomass, and MB loaded.

3.2. Adsorption studies

3.2.1. Effect of solution pH

The influence of pH on adsorption efficiency has been studied and reported (Ho, 2005; Metin *et al.*, 2020; Shahnaz *et al.*, 2022). pH affects the ionization degree of the functional groups on the biosorbent surface. Adsorption of MB by the green microalga *S. regularis* was first investigated by the initial pH level of the dye solution (Figure 4a). The adsorption capacity increased 3.5 times when the aqueous solution pH values increased to the 2-6 range. Nonetheless, the adsorption capacity of *S. regularis* did not change significantly in the pH range of 6-10; the adsorption capacity increased from 42.39 to 45.32 mg/g. This wide pH range where high capacity is found provides a significant advantage since freshwater pH values are generally at the basic level (Alver *et al.*, 2020). The acidic condition at low pH results in a high number of H$^+$ ions, decreasing dye removal by the biosorbent. However, cationic dyes ionize, and load positively charged ions into

aqueous solutions (Peydayesh and Rahbar-Kelishami, 2015). Thus, at lower pH levels, protonation of the microalgae surface prevents adsorption of MB onto the biosorbent mainly through electrostatic repulsion and competition between H^+ ions and cationic dye molecules for the adsorption sites. As the initial pH levels increase to basic pH values, the number of H^+ decreases, while those of OH^- increase, allowing the negatively charged surface of microalgae to adsorb more MB. After establishing neutral pH conditions, adsorption of cationic dyes through attractions by electrostatic forces is driven (Kankılıç et al., 2016; Rangabhashiyam et al., 2018; Tanhaei et al., 2019). All other experiments were carried out using distilled water at pH = 6.8.
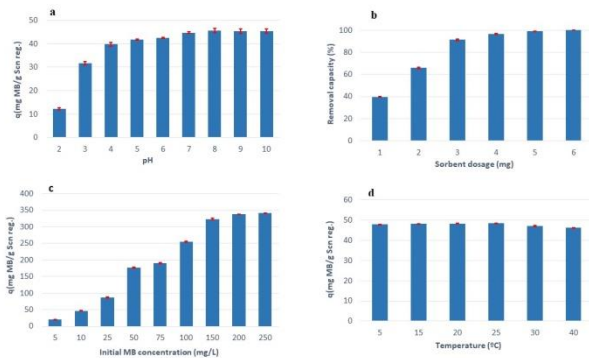

Figure 4. a) The pH profile of MB biosorption on *S. regularis*; *V*= 25 mL; *W*= 0.005 g; *C_{MB}*= 10 mg/L; *T* = 25 °C; b) The effect of sorbent dosage on methylene blue adsorption onto *S. regularis; C_{MB}*= 10 mg/L; *pH*=6.8; *V*=25 mL; *T*= 25 °C; c) The effect of initial MB concentration on removal capacity of *S. regularis; V*= 25 mL; *W_{PA}*= 0.005 g; *pH*=6.8; *T*= 25 °C; d) The effect of temperature on dye removal capacity of *S. regularis*; *W*= 0.005 g; *V*= 25 mL, *pH*= 6.8; *C_{MB}*= 10 mg/L.

3.2.2. Effect of the biosorbent dosage

The effect of the biosorbent concentration on MB removal was studied at a constant dye concentration (10 mg/L), while the biosorbent concentration was changed. The biosorbent dosage was changed between 1 and 6 mg. The biosorbent dosage increased the MB removal efficiency (Figure 4b). The increase in biosorbent dosage from 1 mg to 6 mg increased removal efficiency from 39.71 to 100%. It is seen that increasing the biosorbent dosage reveals more available active sites on the biosorbent surface and

surface area for dye molecules (Nair et al., 2014; Rangabhashiyam et al., 2018; Shahnaz et al., 2022). However, the adsorption capacity of *S. regularis* decreased from 97.23 to 40.50 mg/g with increasing biosorbent dosage. The lower adsorption capacity with a higher biosorbent dosage was because of the constant dye concentrations and unsaturated biosorbent sites. In addition, the increased biosorbent dosage may have caused biomass aggregation and decreased adsorption capacity (Alencar et al., 2012; Aravindhan et al., 2007). Finally, a biosorbent dosage of 5 mg was designated the optimum biosorbent dosage and employed in the experiments.

3.2.3. Effect of initial dye concentration and isotherm studies

The influence of the initial MB concentration on adsorption capacity is shown in Figure 4c. As expected, adsorption capacity increased with increasing initial MB concentration. The amount of adsorbed MB on the biomass increased from 20.46 to 341.34 mg/g, increasing the MB concentration from 5 to 250 mg/L. An increase in initial dye concentration is a substantial driving force to come through all oppositions of the dye between the aqueous and solid phases, thereby resulting in increased adsorption of MB (Alver et al., 2020; Aravindhan et al., 2007; Peydayesh and Rahbar-Kelishami, 2015). In agreement with studies by Kankılıç et al. (2016) and Shooto et al. (2020), this situation can be explained by the presence of a significant number of adsorption binding sites over the initial stage of the adsorption process. The adsorption capacity of *S. regularis* under laboratory conditions is compared with different plant-based biosorbents in Table 1. Defatted *Laminaria japonica* biomass, modified with sulfuric acid, showed a higher removal capacity than *Scenedesmus regularis* (Shao et al., 2017). Considering the amount of Laminaria japonica biomass used, it has been seen that the amount of biosorbent used in this study (0.6 g/L) was considerably higher than in our study (5 mg/L). As seen from the table, *Scenedesmus regularis* has a high adsorption capacity. We recommend it as a good candidate for MB removal due to its considerably high capacity without any modification.

Table 1. Comparison of MB biosorption capacity of *S. regularis* with other microalgae- and plant-based biosorbents

Sorbent	q_m (mg/g)	References
Phragmites australis (modified)	46.8	(Kankılıç et al., 2016)
Spirodela polyrhiza	119	(Waranusantigul et al., 2003)
Chlorella pyrenoidosa	101.75	(Lebron et al., 2018)
Spirulina maxima	145.34	(Lebron et al., 2018)
Raw *Spirogyra sp.*	50.70	(Guler and Sarioglu, 2013)
Pretreated *Spirogyra sp.*	64.61	(Guler and Sarioglu, 2013)
Scenedesmus sp.	87.69	(Afshariani and Roosta, 2019)
Chlorella pyrenoidosa	31.15	(Pathak et al., 2015)
Scenedesmus sp.	6.0	(Sarat Chandra et al., 2015)
Defatted *Scenedesmus sp.*	7.73	(Sarat Chandra et al., 2015)
Sulfuric acid pretreated *Scenedesmus* DAB	7.80	(Sarat Chandra et al., 2015)
Defatted *Laminaria japonica* (Sulfuric acid modified)	549.45	(Shao et al., 2017)
Scenedesmus regularis	341.34	Current study

Table 2. Isotherm constants for MB biosorption by *Scenedemus regularis* according to various isotherm models

Isotherm model	Expression formula	Model parameters		
		$K_L *10^3$ (L/mg)	q_m (mg/g)	R^2
Langmiur	$1/q_e = 1/q_m + 1/q_m K_L C_e$	6.95	625	0.994
		K_F	n	R^2
Freundlich	$\ln q_e = \ln K_F + (1/n)\ln C_e$	8.06	1.38	0.972
		E(kj/mol)	Q_{D-R}(mg/g)	R^2
Dubinnin-Raduskevich	$\ln q_e = K\varepsilon^2 + \ln q_{D-R}$ $\varepsilon = RT \ln (1 + 1/C_e)$ $E = 1/(-2K)^{1/2}$	5.0	469.80	0.993

q_m: maximum biosorption capacity (mg/g), K_L: Langmuir constant (L/mg), K_F (mg/g (L/mg)$^{1/n}$) and n: Freundlich constants, Q_{D-R}: biosorption capacity of Dubinin–Radushkevich (mg/g), ε: Polanyi potential (kJ^2/mol^2), K: Dubinin–Radushkevich, constant, E: free energy (kJ/mol), R: universal gas constant (8.314 J/mol K), T: working temperature (K)

Adsorption isotherm models are extensively used to assess the surface properties of biosorbents and adsorption behavior and to design real adsorption systems (Alver *et al.*, 2020). To investigate the MB adsorption behavior by the biosorbent, experimental data were evaluated with Langmuir, Freundlich, and Dubinin Radushkevich isotherm models. These three isotherm models are widely used, and details are provided in the literature (Kankılıç *et al.*, 2016; Lebron *et al.*, 2018; Metin *et al.*, 2020).

The adsorption isotherm formulae and calculated model parameters are given in Table 2 (Alver *et al.*, 2020; Koyuncu and Kul, 2020; Shayesteh *et al.*, 2016). In the mathematical formulae, C_e (mg/L) is the MB concentration of the aqueous solution at equilibrium, and q_{max} and Q_{D-R} are the maximum MB uptake (mg/g). The three isotherm models are preferred for explaining the adsorption behavior of the dyes (Koyuncu and Kul, 2020; Lebron *et al.*, 2018; Rangabhashiyam *et al.*, 2018).

According to the correlation coefficient (R^2) values obtained from the three isotherm models, the adsorption process of MB fits both the Langmuir and Dubinin Radushkevich models due to the high and almost identical R^2 values of 0.994 and 0.993, respectively. Therefore, the adsorption process of MB onto *Scenedesmus regularis* was better explained by the Langmuir isotherm, i.e., The adsorption mainly occurs as a monolayer on the surface (Kankılıç *et al.*, 2016; Lebron *et al.*, 2018). According to the Langmuir and D-R isotherms, the maximum experimental adsorption capacity is lower than the calculated maximum adsorption capacity (Table 2). This circumstance may be ascribed to incomplete MB contact with algal biomass (Kankılıç *et al.*, 2016; Alver *et al.*, 2020). The K_L value is the Langmuir constant and refers to the affinity between the dye molecules and biosorbent. If the K_L value is high, it shows a high affinity of the dye molecules to the biosorbent, similar to our results (Table 2).

At the same time, the D-R isotherm model is used to elucidate whether the adsorption process of MB is physical or chemical. The E value calculated from the D-R isotherm model indicates the type of adsorption process: if the E value is between 1-8 kJ/mol, then the adsorption process is considered physical. On the other hand, when the E value is between 8-16 kJ/mol, the process is chemical (Chen *et al.*, 2019; Lebron *et al.*, 2018). The calculated E value was found to be 5.0 kJ/mol (less than 8 kJ/mol), so the adsorption of MB onto *Scenedesmus regularis* was attributed to physical adsorption (Table 2).

Moreover, the adsorption process was evaluated with the separation factor (R_L) of the Langmuir isotherm to decide whether the process was favorable or unfavorable. The following equation calculates the RL value:

$$R_L = \frac{1}{1 + K_L C_0} \tag{6}$$

where C_0 is the initial concentration of MB (mg/L) and K_L is the Langmuir constant (L/mg). According to the R_L values, the adsorption process is defined as favorable (between 0-1), irreversible (R_L=0), linear (R_L=1), and undesirable (R_L>1) (Lebron *et al.*, 2018; Mohebali *et al.*, 2018; Shayesteh *et al.*, 2016). Our calculated R_L values for all initial concentrations were between 0.36-0.94, leading us to conclude that the adsorption process was favorable for algal biomass.

3.2.4. Effect of contact time and kinetic studies

Figure 5a shows the effect of contact time on the adsorption of MB onto *S. regularis* biomass. The adsorption rate was very rapid within the first ten minutes. Approximately 92% of the dye was removed within two minutes, and the removal percentage reached 99% within 15 minutes, after this point, no significant difference was found.

Adsorption kinetics must be well known to determine the adsorption rate, the productivity of the sorbent used, and mass transfer mechanisms. The rate and degree of a reaction depend on the number of molecules that will react to produce the product and the reaction kinetics. Therefore, the determination of adsorption kinetics is fundamental for the envisagement of adsorption systems (Wang and Guo, 2020). Adsorption kinetics were evaluated using pseudo-first-order and pseudo-second-order kinetic models (Shayesteh *et al.*, 2016; Metin *et al.*, 2020). The expression formulae of the kinetic models and calculated parameters are given in Table 3. These parameters were calculated from the slope and intercept of the pseudo-first-order kinetic model and pseudo-second-order kinetic model (Figure 5b and 5c).

Table 3. Calculated kinetic parameters for pseudo-first-order and pseudo-second-order models for methylene blue biosorption using *Scenedesmus regularis* (T: 298 K, C_e: 10 mg/L; sorbent dosage: 0.006 g biomass)

Kinetic model	Expression Formula	Parameters	MB
Pseudo-first-order	$\log(qe - qt) = \log qe - \left(\dfrac{k_1 t}{2.303}\right)$	$q_{e,cal}$ (mg/g)	3.61
		$q_{e,\,exp}$ (mg/g)	46.64
		k_1 (min^{-1})	0.196
		R^2	0.9417
Pseudo-second-order	$\dfrac{t}{qt} = \dfrac{1}{k_2 q_e^2} + \dfrac{t}{q_e}$	$q_{e,cal}$ (mg/g)	46.73
		$q_{e,\,exp}$ (mg/g)	46.64
		k_2 (g mg^{-1} min^{-1})	0.382
		R^2	0.9994

Table 4. Thermodynamic parameters for the biosorption of methylene blue *on Scnedesmus regularis*

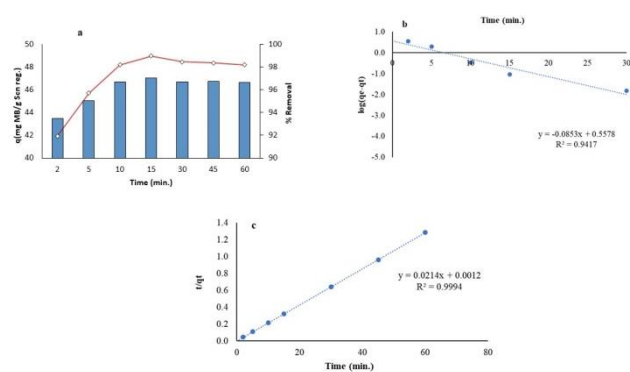| Temperature (K)	ΔG°(kj/mol)	ΔH° (j/mol)	ΔS° (j/molK)	TΔS° (kj/mol)	R^2
278	-5.23			5.60	
288	-5.43			5.81	
293	-5.53	377.88	20.16	5.91	0.994
298	-5.63			6.01	
303	-5.73			6.11	
313	-5.93			6.31	

Figure 5. a) Effect of contact time for biosorption of MB on *S. regularis*; *V*= 25 mL; *pH*= 6.8; *W*=0.005 g; C_{MB}= 10 mg/L; *T*= 25 °C; b) Pseudo-first order; c) Pseudo-second-order kinetic plot for the removal of MB by *S. regularis*; *T*: 298 K; C_o: 10 mg/L.

According to the R^2 values, the pseudo-second-order model has a higher correlation coefficient than the pseudo-first-order model (Table 3). The calculated adsorption capacity (q_{ecal}) calculated from the pseudo-second-order model was in accord with the experimental adsorption capacity (q_{eexp}). The parameters showed that the adsorption process was controlled with a pseudo-second-order kinetic model. Research has shown that the pseudo-second-order kinetic model exhibits better agreement with experimental data than the other model and therefore is widely used in kinetic studies (Lebron *et al.*, 2018). Similar results for dye adsorption have been presented in the literature (Khataee *et al.*, 2013; Metin *et al.*, 2020; Mitrogiannis *et al.*, 2015; Shao *et al.*, 2017; Wang *et al.*, 2018).

3.2.5. Effect of temperature and thermodynamic studies

One of the essential parameters is temperature, which affects the adsorption capacity of the biosorbent and the transport and kinetic process of adsorbate molecules (Kankılıç *et al.*, 2016). Therefore, the effect of temperature was investigated between 5-40 °C. As shown in Figure 4d, the adsorption capacity was approximately the same with increasing temperature. The differences between temperatures were not significant. After 25 °C, the adsorption capacity imperceptibly decreased.

This situation shows that the temperature has too little effect on the adsorption process. Similar results have been given in the literature regarding the effect of temperature on MB removal (Gemici *et al.*, 2021; Kankılıç *et al.*, 2016).

Thermodynamic parameters such as Gibbs free energy (ΔG°), enthalpy (ΔH°), and entropy (ΔS°) values were used to elaborate the adsorption process (Gemici *et al.*, 2021; Lebron *et al.*, 2018) and were calculated as in our previous work (Kankılıç *et al.*, 2016; Kankılıç *et al.*, 2020). As seen in Table 4, negative ΔG° values for all temperatures indicated a spontaneous and suitable adsorption process (Gemici *et al.*, 2021; Gokulan *et al.*, 2022b Shooto *et al.*, 2020). The negative ΔG° values of the reaction illustrate that the adsorption process required no energy input from an outside source(s) (Mitrogiannis *et al.*, 2015).

The positive ΔH° value (377 J/mol) shows that MB adsorption onto algal biomass is endothermic, and if this value is less than 40 kJ/mol, the adsorption process is physisorption (Kasperiski *et al.*, 2018). In addition, the positive ΔS° value indicates randomness in the adsorption process and good affinity to microalgal biomass (Gemici *et al.*, 2021; Kankılıç *et al.*, 2016).

4. Conclusion

This study pointed out that *Scenedesmus regulari*s can make used as a highly effective, low-cost, eco-friendly biosorbent and is an important alternative for methylene blue removal from polluted aquatic systems without any chemical modification. The results of our experiments

showed that the adsorption process was barely affected by temperature and that a high adsorption capacity was achieved over a wide pH range. The maximum experimental adsorption capacity was 341.34 mg/g of dry biomass at an MB concentration of 250 mg/L, an algal biomass dosage of 0.005 g, an initial pH of 6.8, and a temperature of 25 °C. The adsorption process was rapid; 92% of MB was removed within two minutes, and equilibrium was achieved in fifteen minutes. Isotherm studies demonstrated that the Langmuir isotherm model and Dubinin Raduskevich were well fitted by adsorption equilibrium. As a result of isotherm studies, the adsorption process was monolayer and of physical type. Thermodynamic calculations showed that the adsorption process was endothermic, spontaneous, and favorable.

Ethics approval and consent to participate

Not applicable.

Consent to Participate

Not applicable.

Consent for publication

Not applicable.

Authors' contributions

Gökben Başaran Kankılıç: Conceptualization, Methodology, Investigation, Laboratory experiments, Formal analysis, Writing original draft, Writing – review & editing.

Competing of interests

The author declares that she has no known competing financial interests or personal relationships that could have appeared to influence the work reported in this paper.

References

Afshariani F. and Roosta A. (2019), Experimental study and mathematical modeling of biosorption of methylene blue from aqueous solution in a packed bed of microalgae Scenedesmus, *Journal of Cleaner Production,* **225**, 133–142.

Ahmad A., Mohd-Setapar S.H., Chuong C.S., Khatoon A., Wani W.A., Kumar R. and Rafatullah M. (2016), Recent advances in new generation dye removal technologies: Novel search for approaches to reprocess wastewater, *RSC Advances*, **6,** 10430.

Ahmad A., Rafatullah M., Sulaiman O., Ibrahim M.H. and Hashim R. (2009), Scavenging behaviour of meranti sawdust in the removal of methylene blue from aqueous solution, *Journal of Hazardous Materials*, **170**, 357–365.

Alencar W.S., Acayanka E., Lima E.C., Royer B., de Souza F.E., Lameira J. and Alves C.N. (2012), Application of Mangifera indica (mango) seeds as a biosorbent for removing Victazol Orange 3R dye from aqueous solution and studying the biosorption mechanism, *Chemical Engineering Journal,* **209**, 577–588.

Alipanahpour Dil E., Ghaedi M., Ghezelbash G.R., Asfaram A. and Purkait M.K. (2017), Highly efficient simultaneous biosorption of Hg2+, Pb2+ and Cu2+ by Live yeast Yarrowia lipolytica 70562 following response surface methodology optimization: Kinetic and isotherm study. *Journal of Industrial and Engineering Chemistry*, **48**, 162–172.

Alver E., Metin A.Ü. and Brouers F. (2020), Methylene blue adsorption on magnetic alginate/rice husk bio-composite, *International Journal of Biological Macromolecules* **154**, 104–113.

Aravindhan R., Rao J.R. and Nair B.U. (2007), Removal of basic yellow dye from aqueous solution by sorption on green alga Caulerpa scalpelliformis, *Journal of Hazardous Materials,* **142**, 68–76.

Baruah S., Devi A., Bhattacharyya K.G. and Sarma A. (2017), Developing a biosorbent from Aegle Marmelos leaves for removal of methylene blue from water. *International Journal of Environmental Science and Technology,* **14**, 341–352.

Chen S., Qin C., Wang T., Chen F., Li X., Hou H. and Zhou M. (2019), Study on the adsorption of dyestuffs with different properties by sludge-rice husk biochar: Adsorption capacity, isotherm, kinetic, thermodynamics and mechanism, *Journal of Molecular Liquids* **285**, 62–74.

Dahri M.K., Kooh M.R.R. and Lim L.B.L. (2015), Application of Casuarina equisetifolia needle for the removal of methylene blue and malachite green dyes from aqueous solution. *Alexandria Engineering Journal,* **54**, 1253–1263.

Daneshvar E., Vazirzadeh A., Niazi A., Kousha M., Naushad M. and Bhatnagar A. (2017), Desorption of Methylene blue dye from brown macroalga: Effects of operating parameters, isotherm study and kinetic modeling, *Journal of Cleaner Production*, **152**, 443–453.

Gemici B.T., Ozel H.U. and Ozel H.B. (2021), Removal of methylene blue onto forest wastes: Adsorption isotherms, kinetics and thermodynamic analysis, *Environmental Technology & Innovation*, **22**, 101501.

Gokulan R., Ganesh Prabhu G., Avinash A., Jegan J. (2020), Experimental and chemometric analysis of bioremediation of remazol dyes using biochar derived from green seaweeds. *Desalination WATER Treatment*, **184**, 340–353.

Gokulan R., Kalyani G., Killi S. (2022a), Removal of Reactive Red 120 in a Batch Technique Using Seaweed-Based Biochar: A Response Surface Methodology Approach. *Journal of Nanomaterials,* **2022**, 1–12.

Gokulan R., Ganesh Prabhu G., Avinash A., Saravanan S. (2022b). Soft computing-based models and decolorization of Reactive Yellow 81 using Ulva Prolifera biochar, *Chemosphere*, **287**(4), 132368.

Gualtieri P. and Barsanti L. (2006), Algae : anatomy, biochemistry, and biotechnology. Taylor & Francis.

Guler U.A. and Sarioglu M. (2013), Single and binary biosorption of Cu(II), Ni(II) and methylene blue by raw and pretreated Spirogyra sp.: Equilibrium and kinetic modeling, *Journal of Environmental Chemical Engineering*, **1**, 369–377.

Ho Y.S. (2005), Effect of pH on lead removal from water using tree fern as the sorbent. *Bioresource Technology,* **96**, 1292–1296.

Kabra A.N., Khandare R.V., Waghmode T.R. and Govindwar S.P. (2011), Differential fate of metabolism of a sulfonated azo dye Remazol Orange 3R by plants Aster amellus Linn., Glandularia pulchella (Sweet) Tronc. and their consortium, *Journal of Hazardous Materials,* **190**, 424–431.

Kankılıç G.B., Metin A.Ü. and Tüzün I. (2016). Phragmites australis: An alternative biosorbent for basic dye removal, *Ecological Engineering*, **86**, 85–94.

Kankılıç G.B., Metin A.Ü. and Aluç Y. (2020), Investigation on phenol degradation capability of Scenedesmus regularis:

influence of process parameters, *Environmental Technology (United Kingdom)*, **41**, 1065–1073.

Kasperiski F.M., Lima E.C., Umpierres C.S., dos Reis G.S., Thue P.S., Lima D.R., Dias S.L.P., Saucier C. and da Costa J.B. (2018), A Production of porous activated carbons from Caesalpinia ferrea seed pod wastes: Highly efficient removal of captopril from aqueous solutions, *Journal of Cleaner Production,* **197**, 919–929.

Khataee A.R., Vafaei F. and Jannatkhah M. (2013), Biosorption of three textile dyes from contaminated water by filamentous green algal Spirogyra sp.: Kinetic, isotherm and thermodynamic studies, *International Biodeterioration & Biodegradation*, **83**, 33–40.

Koyuncu H. and Kul A.R. (2020), Removal of methylene blue dye from aqueous solution by nonliving lichen (Pseudevernia furfuracea (L.) Zopf.), as a novel biosorbent, *Applied Water Science*, **10**, 72.

Kumar S.S., Balasubramanian P. and Swaminathan G. (2013), Degradation potential of free and immobilized cells of white rot fungus Phanerochaete chrysosporium on synthetic dyes, International Journal of ChemTech Research, **5**, 565–571.

Lebron Y.A.R., Moreira V.R., Santos L.V.S. and Jacob R.S. (2018), Remediation of methylene blue from aqueous solution by Chlorella pyrenoidosa and Spirulina maxima biosorption: Equilibrium, kinetics, thermodynamics and optimization studies, *Journal of Environmental Chemical Engineering*, **6**, 6680–6690.

Low L.W., Teng T.T., Ahmad A., Morad N. and Wong Y.S. (2011), A novel pretreatment method of lignocellulosic material as adsorbent and kinetic study of dye waste adsorption, Water, Air, Soil Pollution, **218**, 293-306.

Metin A.Ü., Doğan D. and Can M. (2020), Novel magnetic gel beads based on ionically crosslinked sodium alginate and polyanetholesulfonic acid: Synthesis and application for adsorption of cationic dyes, *Materials Chemistry and Physics*, 256, 123659.

Mitrogiannis D., Markou G., Çelekli A. and Bozkurt H. (2015), Biosorption of methylene blue onto Arthrospira platensis biomass: Kinetic, equilibrium and thermodynamic studies, *Journal of Environmental Chemical Engineering*, **3**, 670–680.

Mohebali S., Bastani D., Shayesteh H. (2018), Methylene blue removal using modified celery (Apium graveolens) as a low-cost biosorbent in batch mode: Kinetic, equilibrium, and thermodynamic studies, *Journal of Molecular Structure*, **1173**, 541-551.

Naghipour D., Taghavi K. and Moslemzadeh M. (2016), Removal of methylene blue from aqueous solution by Artist's Bracket fungi: Kinetic and equilibrium studies, *Water Science And Technology*, **73**, 2832–2840.

Nair V., Panigrahy A. and Vinu R., 2014. Development of novel chitosan-lignin composites for adsorption of dyes and metal ions from wastewater, *Chemical Engineering Journal*, **254**, 491–502.

Pathak V.V., Kothari R., Chopra A.K. and Singh D.P. (2015), Experimental and kinetic studies for phycoremediation and dye removal by Chlorella pyrenoidosa from textile wastewater. *Journal of Environmental Management,* **163**, 270–277.

Peydayesh M. and Rahbar-Kelishami A. (2015), Adsorption of methylene blue onto Platanus orientalis leaf powder: Kinetic, equilibrium and thermodynamic studies. *Journal of Industrial and Engineering Chemistry*, 21, 1014–1019.

Phinyo K., Pekkoh J., Peerapornpisal Y. (2017), Distribution and ecological habitat of Scenedesmus and related genera in some

freshwater resources of Northern and North-Eastern Thailand. *Biodiversitas*, 18, 1092-1099.

Rafatullah M., Sulaiman O., Hashim R. and Ahmad A. (2010). Adsorption of methylene blue on low-cost adsorbents: A review, *Journal of Hazardous Materials,* **1-3**, 70-80.

Rahman H.L., Erdem H., Sahin M. and Erdem M. (2020), Iron-Incorporated Activated Carbon Synthesis from Biomass Mixture for Enhanced Arsenic Adsorption, Water Air Soil Pollution, **231**, 6.

Rajasulochana P. and Preethy V. (2016), Comparison on efficiency of various techniques in treatment of waste and sewage water – A comprehensive review, *Resource-Efficient Technologies*, **2**, 175–184.

Rangabhashiyam S., Lata S. and Balasubramanian P. (2018), Biosorption characteristics of methylene blue and malachite green from simulated wastewater onto Carica papaya wood biosorbent. Surfaces and Interfaces, **10**, 197–215.

Ravikumar K., Deebika B. and Balu K. (2005), Decolourization of aqueous dye solutions by a novel adsorbent: Application of statistical designs and surface plots for the optimization and regression analysis, *Journal of Hazardous Materials*, **122**, 75–83.

Saha P., Chowdhury S.and Tadashi M. Eds. (2011), Insight into Adsorption Thermodynamic, pp. 349–364, IntechOpen, London, UK, 2011, Chapter 16.

Sarat Chandra T., Mudliar S.N., Vidyashankar S., Mukherji S., Sarada R., Krishnamurthi K. and Chauhan V.S. (2015), Defatted algal biomass as a non-conventional low-cost adsorbent: Surface characterization and methylene blue adsorption characteristics. *Bioresource Technology,* **184**, 395–404.

Sari A., Uluozlü Ö.D. and Tüzen M. (2011), Equilibrium, thermodynamic and kinetic investigations on biosorption of arsenic from aqueous solution by algae (Maugeotia genuflexa) biomass. Chemical Engineering Journal, **167**, 155–161.

Shahnaz T., Bedadeep D. and Narayanasamy S. (2022), Investigation of the adsorptive removal of methylene blue using modified nanocellulose. *International Journal of Biological Macromolecules*, **200**, 162–171.

Shao H., Li Y. and Zheng L., Chen T. and Liu J. (2017). Removal of methylene blue by chemically modified defatted brown algae Laminaria japonica. *Journal of the Taiwan Institute of Chemical Engineers,* **80**, 525–532.

Shayesteh H., Rahbar-Kelishami A. and Norouzbeigi R. (2016), Evaluation of natural and cationic surfactant modified pumice for congo red removal in batch mode: Kinetic, equilibrium, and thermodynamic studies, *Journal of Molecular Liquids*, **221**, 1–11.

Shooto N.D., Naidoo E.B. and Maubane M. (2019), Sorption studies of toxic cations on ginger root adsorbent, *Journal of Industrial and Engineering Chemistry*, **76**, 133–140.

Shooto N.D., Thabede P.M., Bhila B., Moloto H. and Naidoo E.B. (2020), Lead ions and methylene blue dye removal from aqueous solution by mucuna beans (velvet beans) adsorbents, *Journal of Environmental Chemical Engineering*, **8**, 103557.

Stavrinou A., Aggelopoulos C.A. and Tsakiroglou C.D. (2018), Exploring the adsorption mechanisms of cationic and anionic dyes onto agricultural waste peels of banana, cucumber and potato: Adsorption kinetics and equilibrium isotherms as a tool. *Journal of Environmental Chemical Engineering*, **6**, 6958–6970.

Tanhaei B., Ayati A. and Sillanpää M. (2019), Magnetic xanthate modified chitosan as an emerging adsorbent for cationic azo dyes removal: Kinetic, thermodynamic and isothermal

studies, *International Journal of Biological Macromolecules*, **121**, 1126–1134.

Wang J. and Guo X. (2020), Adsorption kinetic models: Physical meanings, applications, and solving methods, *Journal of Hazardous Materials*, **390**, 122156.

Wang P., Tang Y., Liu Y., Wang T., Wu P. and Lu X.Y. (2018), Halloysite nanotube@carbon with rich carboxyl groups as a multifunctional adsorbent for the efficient removal of cationic Pb(ii), anionic Cr(vi) and methylene blue (MB), *Environmental Science: Nano*, **5**, 2257–2268.

Wang S., Boyjoo Y., Choueib A. and Zhu Z.H. (2005), Removal of dyes from aqueous solution using fly ash and red mud, *Water Research*, **39**, 129–138.

Waranusantigul P., Pokethitiyook P., Kruatrachue M. and Upatham E.S. (2003), Kinetics of basic dye (methylene blue) biosorption by giant duckweed (Spirodela polyrrhiza), *Environmental Pollution*, **125**, 385–392.